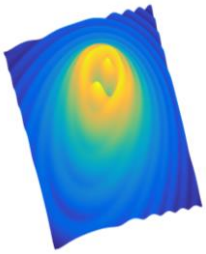

DOING PHYSICS WITH MATLAB

COMPUTATIONAL OPTICS

RAYLEIGH-SOMMERFELD DIFFRACTION INTEGRAL OF THE FIRST KIND

ILLUMINATION OF A CIRCULAR APERTURE BY A POINT SOURCE

Ian Cooper School of Physics University of Sydney
ian.cooper@sydney.edu.au

DOWNLOAD DIRECTORY FOR MATLAB SCRIPTS

It is necessary to modify the mscripts and comment or uncomment lines of code to run the simulations with different input and output parameters.

op_rs_point_source.m

Calculation of the irradiance in a plane perpendicular to the optical axis for a circular aperture illuminated by a point source on the optical axis. It uses Method 3: one-dimensional form of Simpson's rule for the integration of the diffraction integral.

op_rs_point_sources_z.m

Calculation of the irradiance along the optical axis for a circular aperture illuminated by a point source on the optical axis. It uses Method 3: one-dimensional form of Simpson's rule for the integration of the diffraction integral.

op_rs_point_sources_xz.m

Calculation of the irradiance in the meridional - XZ plane for a circular aperture illuminated by a point source on the optical axis. It uses Method 3: one-dimensional form of Simpson's rule for the integration of the diffraction integral.

op_rs_point_sources_xy.m

Calculation of the radial irradiance for a circular aperture illuminated by a point source on the optical axis or located off the optical axis. It uses Method 3: one-dimensional form of Simpson's rule for the integration of the diffraction integral. This mscript runs slower than the others because you can't make use of the circular symmetry because the source can be located off-axis.

Function calls to:

simpson1d.m (integration)

fn_distancePQ.m (calculates the distance between points P and Q)

turningPoints.m (finds the location of zeros, min and max of function)

Warning: The results of the integration may look OK but they may not be accurate if you have used insufficient number of partitions for the aperture space and observation space. It is best to check the convergence of the results as the number partitions is increased. Note: as the number of partitions increases, the calculation time **rapidly** increases.

RAYLEIGH-SOMMERFELD DIFFRACTION INTEGRAL OF THE FIRST KIND

The Rayleigh-Sommerfeld diffraction integral of the first kind states that the electric field E_P at an observation point P can be expressed as

$$(1) \qquad E_P = \frac{1}{2\pi} \iint_{S_A} E(\vec{r}) \frac{e^{jkr}}{r^3} z_p (jkr - 1)\, \mathrm{d}S \qquad \textit{planar aperture space}$$

It is assumed that the Rayleigh-Sommerfeld diffraction integral of the first kind is valid throughout the space in front of the aperture, right down to the aperture itself. There are no limitations on the maximum size of either the aperture or observation region, relative to the observation distance, because **no approximations have been made**.

The diffraction pattern can be given in terms of the irradiance distribution w_e , where

$$(2) \qquad w_e = \frac{n \varepsilon_0 c}{2} E_P^{\,*} E_P \qquad [\mathrm{W.m^{-2}}]$$

where ε_0 is the permittivity of free space, c is the speed of light in vacuum, n is the refractive index of the medium and E_P is the peak value of the electric field at a point P in the observation space [$\mathrm{V.m^{-1}}$].

The time rate of flow of radiant energy is the **radiant flux** W_E where

$$(3) \qquad W_E = \iint_{area} w_e \, dA \qquad [\mathrm{W \ \ or \ \ J.s^{-1}}]$$

- Numerical Integration Methods for the Rayleigh-Sommerfeld Diffraction Integral of the First Kind
- Irradiance and radiant flux

A CIRCULAR APERTURE ILLUMINATED BY A POINT SOURCE

By numerically integrating the Rayleigh-Sommerfeld integral of the first kind (equation 1), the diffracted wave field can be calculated from the plane of the aperture to the far field without introducing many of the standard approximations that are used to give Fresnel or Fraunhofer diffraction. The geometry for the diffraction by a circular aperture of radius *a* illuminated by a point source is shown in figure (1).

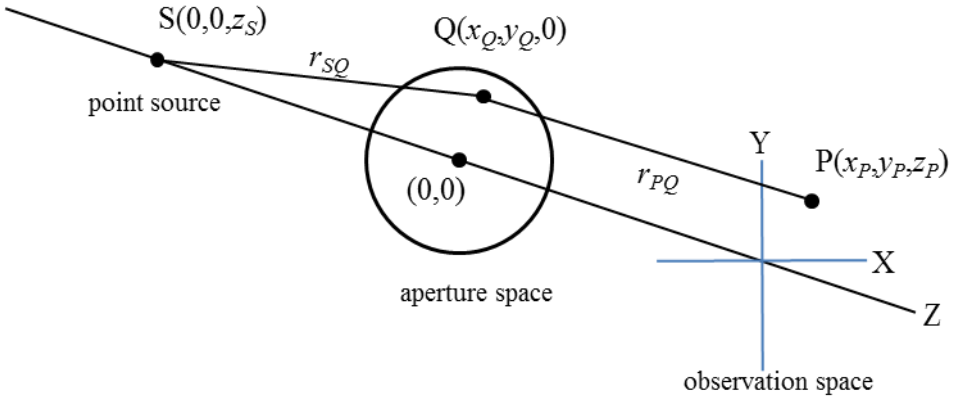

Fig. 1. Geometry for the diffraction by a circular aperture that is illuminated by a point source located on the –Z axis. The radius of the circular aperture is *a*.

The Cartesian coordinates for the source S, an aperture point Q and an observation point P are S(x_S, y_S, z_S), Q(x_Q, y_Q, 0) and P(x_P, y_P, z_P). In using the mscripts **op_rs_point_source.m** or **op_rs_point_source_z.m** the source must be located on the optical axis (Z axis). The distance from the point source S to an aperture point Q is r_{SQ} and the distance from the aperture point to the observation point P is r_{PQ}. The electric field E_Q at an aperture point Q due to the point source S is

$$(2) \qquad E_Q = \frac{E_S \exp\left(j k r_{SQ}\right)}{r_{SQ}}$$

where E_S is the source strength in V.m^{-1}. For the illumination of the circular aperture by the point source, the Rayleigh-Sommerfeld diffraction integral (equation 1) can be expressed as

$$(3) \qquad E_P = \frac{1}{2\pi} \iint_{S_A} \frac{E_S \exp\left(j k r_{SQ}\right)}{r_{SQ}} \frac{\exp\left(j k r_{PQ}\right) e^{jkr}}{r_{PQ}^{\,3}} z_p \left(j k r_{PQ} - 1\right) \mathrm{d}S$$

Equation (3) is evaluated using a one-dimensional form of Simpson's rule. Note: no approximations have been made at this stage. Equation (3) is valid in the entire observation space in front of the aperture. The Rayleigh-Sommerfeld diffraction integral of the first kind gives the "true" diffraction pattern near the aperture, whereas, the Rayleigh-Sommerfeld diffraction integral of the second kind and the Kirchhoff diffraction integral do not.

IRRADIANCE DENSITY VARIATION ALONG THE OPTICAL AXIS

From the Rayleigh-Sommerfeld diffraction integral of the first kind (equation 3), the axial irradiance $I_P(0,0,z_P)$ for a circular aperture illuminated by a plane wave can be expressed in a simple analytical form without any approximations due to the symmetry along the optical axis [Osterberg, Dubra]

(4)

$$I_P(0,0,z_P)=\left(\frac{I_Q}{4}\right)\left(1-\left(\frac{2\,z_P}{\sqrt{a^2+{z_P}^2}}\right)\cos\left(k\left(\sqrt{a^2+{z_P}^2}-z_P\right)\right)+\frac{{z_P}^2}{\sqrt{a^2+{z_P}^2}}\right)$$

where I_Q is the radiant flux density from the aperture. Because of the cosine term, the axial irradiance oscillates and is bound between two envelopes corresponding to the locus of the minima and maxima of the axial irradiance. The envelopes of the peaks and troughs is given by

(5) $$I_P(0,0,z_P)=\left(\frac{I_Q}{4}\right)\left(1\pm\frac{z_P}{\sqrt{{z_P}^2+a^2}}\right)^2$$

From equation (4), peaks in the irradiance distribution along the optical axis will occur when the cosine term is equal to zero, hence

(6) $$k\left(\sqrt{a^2+{z_P}^2}-z_P\right)=(2m+1)\left(\frac{\pi}{2}\right)\qquad m=0,1,2,3,\ldots$$

Rearranging equation (6) gives the values of z_P for the peaks

(7) $$z_P=\frac{a^2-(m+\frac{1}{2})^2\lambda^2}{(2m+1)\lambda}\qquad m=0,1,2,3,\ldots$$

Since $z_P > 0$ then

(8) $$a^2>\left(m+\tfrac{1}{2}\right)^2\lambda^2\quad\Rightarrow\quad m<\frac{a}{\lambda}-\tfrac{1}{2}$$

For an aperture of radius $a = 10\,\lambda$, the allowed values of m are 0, 1, 2, … , 9 giving 10 peak in the irradiance distribution along the optical axis in front of the aperture.

To simulate a plane wave with our point source, it is only necessary to make z_S very large. We will consider a simulation with the following parameters using the mscript **op_rs_point_source_z.m**

Source	$x_S = 0$, $y_S = 0$ and $z_S = -1.00$ m
Source Strength	$E_Q = 1.00$ V.m^{-1}
Wavelength	$\lambda = 632.8$ nm
Aperture radius	$a = 10\ \lambda$
Aperture partitions	$n_Q = 681701$
Observation partitions	$n_P = 1809$

A typical execution time for running the mscript is about 3 minutes.

A comparison of the analytical and numerical evaluations of the diffraction integral (equation 3) is shown in figure (2) – the top graph shows the irradiance from the near field (Fresnel region) to the far field (Fraunhofer region) and the bottom graph shows the near field only. There are 10 peaks in the irradiance distribution as predicted by equation (8). The maximum irradiance occurs at an axial distance of about 100 λ from the aperture and then decreases monotonically with increasing values of z_P. For $z_P <$ 100 λ and as z_P decreases to zero as one approached the aperture, the irradiance oscillates with increasing frequency and decreases in value to ¼ of the maximum irradiance at the largest peak which occurs at about 100 λ.

How good is the Simpson's method of evaluating the diffraction integral given by equation (3) compared with the exact analytical evaluation of the diffraction integral given by equation (4)? The answer is: the agreement between the numerical approach and the analytical one is excellent as shown by the plots in figure (2) provided that the number of partitions of the aperture and observation spaces are sufficiently large. How large can be found by increasing the number of partitions until there is a convergence in the results.

There are often claims in the literature that there are difficulties in performing numerical integration of diffraction integrals because of the highly oscillatory integrand, however, the results as indicated in figure (2), confirms the accuracy of the numerical method using Simpson's rule in evaluating the Rayleigh-Sommerfeld diffraction integral of the first kind.

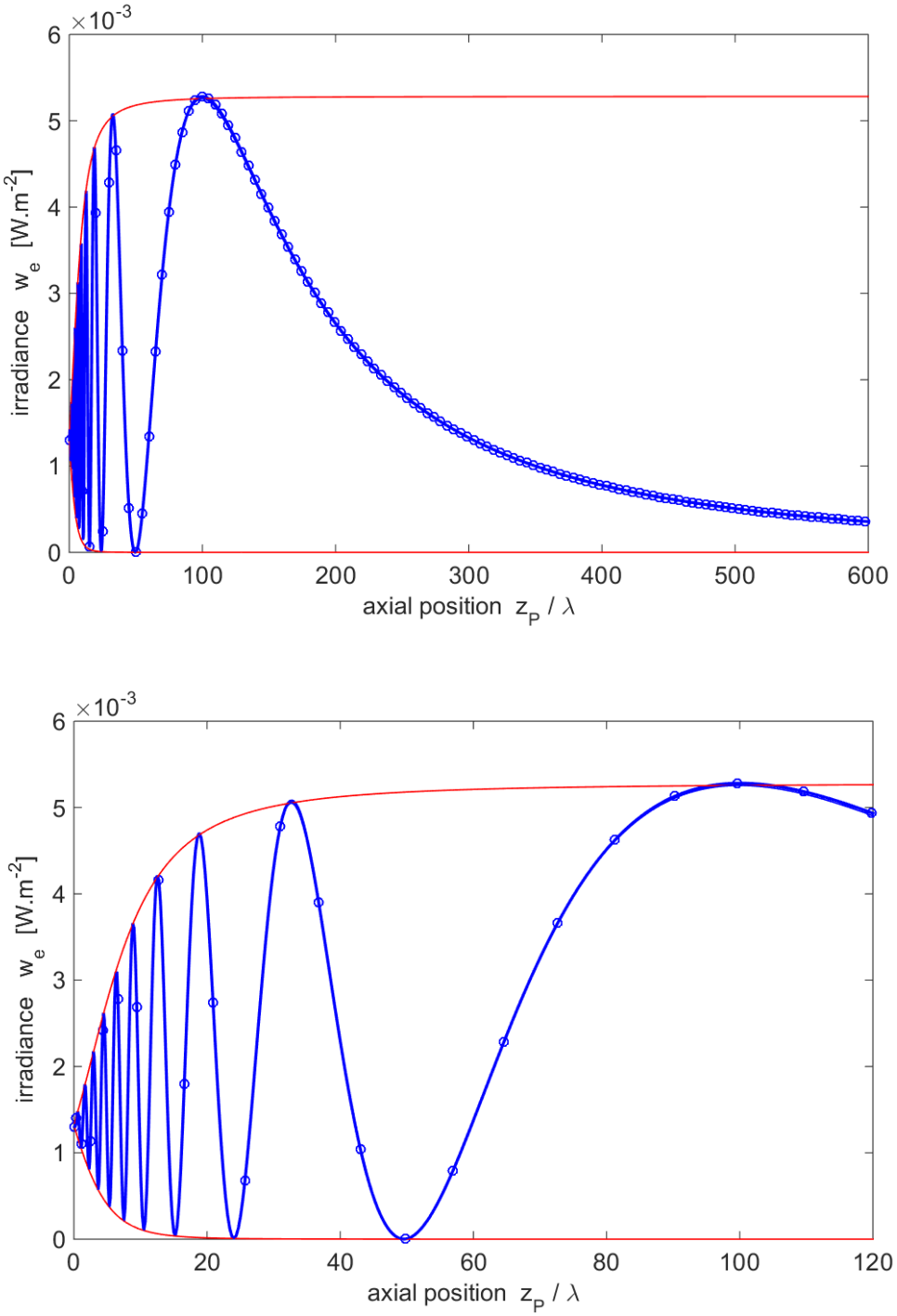

Fig. 2. The irradiance distribution along the optical axis. The red curves are for the envelopes (equation 5), the blue solid curve is the analytical evaluation (equation 4) and the blue circles for the numerical evaluation of equation (3) using Simpson's rule for the double integral.
S(0, 0, - 1.00 m) **op_rs_point_source_z.m**

A numerical approach to evaluating diffraction integrals compared to an analytical one is much more powerful, especially using the Rayleigh-Sommerfeld diffraction integral of the first kind which gives the total diffraction wave field in front of the aperture without the need approximations. An example which it is not possible to do an analytical calculation is shown in figure (3) which shows a plot of the axial irradiance for a point source close to the aperture ($x_S = 0$ $y_S = 0$ $z_S = -50\ \lambda$). The irradiance distribution shown in figure (3) is quite different to the distribution shown in figure (2) for plane wave illumination.

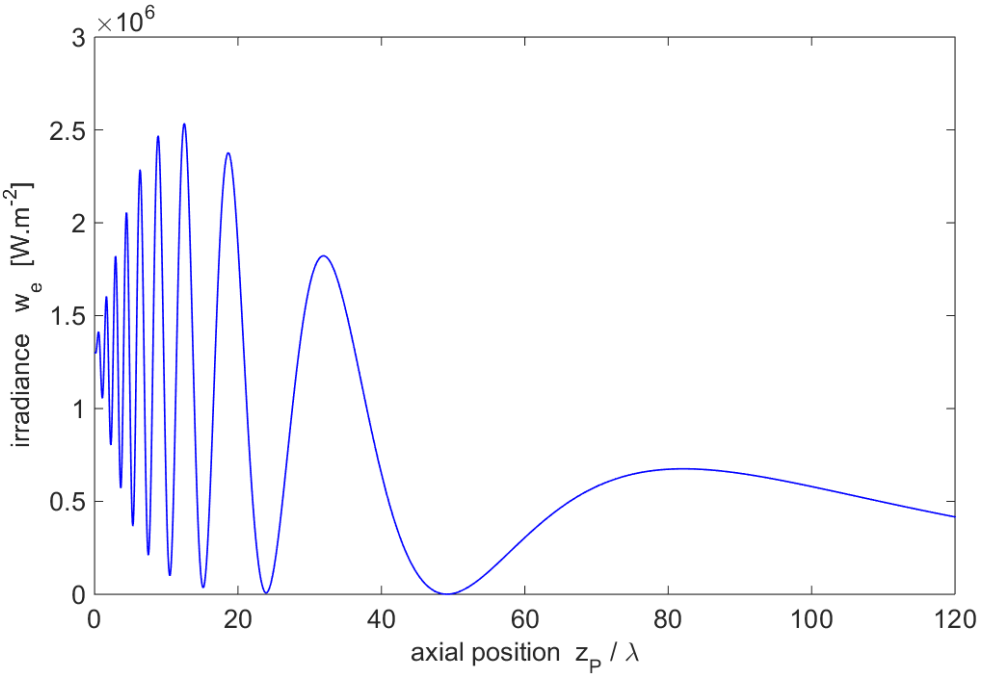

Fig .3. The irradiance distribution along the optical axis for a point source close to the aperture S(0, 0, - 50 λ). **op_rs_point_source_z.m**

IRRADIANCE VARIATION IN A RADIAL DIRECTION

It is only necessary to calculate the irradiance in a radial direction to find the diffraction pattern in a XY observation plane since the diffraction pattern is circularly symmetric when the aperture is illuminated by a point source located on the negative Z axis.

Diffraction patterns in different XY observation planes are shown in figures (4), (5) and (6) when the aperture is illuminated by a point source located far from the aperture and on the optical axis S(0, 0, 1 m). Figure (4) shows the near field (Fresnel diffraction) when the observation plane is close to the aperture, $z_P = 20\,\lambda$. The irradiance distribution is shown in figure (5) when the observation plane is located close to the position of the largest peak on the optical axis ($z_P = 100\,\lambda$). A Fraunhofer diffraction pattern for the far field is shown in figure (6). The diffraction pattern computed numerically agrees with the analytical Fraunhofer equation which gives the shape of the radial diffraction pattern in terms of Bessel functions of the first kind. The radial variation in the irradiance is also shown as a function of the radial optical coordinate v_P which gives a scaled distance from the optical axis.

$$(9) \qquad v_P = \frac{2\pi a}{\lambda}\sin\theta$$

The figures (4), (5) and (6) also show plots of the radiant flux enclosed by circles of increasing radius.

view a more in-depth discussion on the diffraction by circular apertures that are uniformly illuminated (plane wave illumination).

Summary of parameters used in the simulations using the mscript
op_rs_point_source.m

Source S	$x_S = 0$, $y_S = 0$ and $z_S = -1.00$ m
Source Strength	$E_Q = 1.00$ V.m^{-1}
Wavelength	$\lambda = 632.8$ nm
Aperture radius	$a = 10\,\lambda$
Radiant flux from aperture	$W_{eQ} = 1.67\times10^{-13}$ W
Aperture partitions	$n_Q = 481801$
Observation partitions	$n_P = 809$
Rayleigh distance	$d_{RL} = 400\,\lambda$
Execution time	1 minute

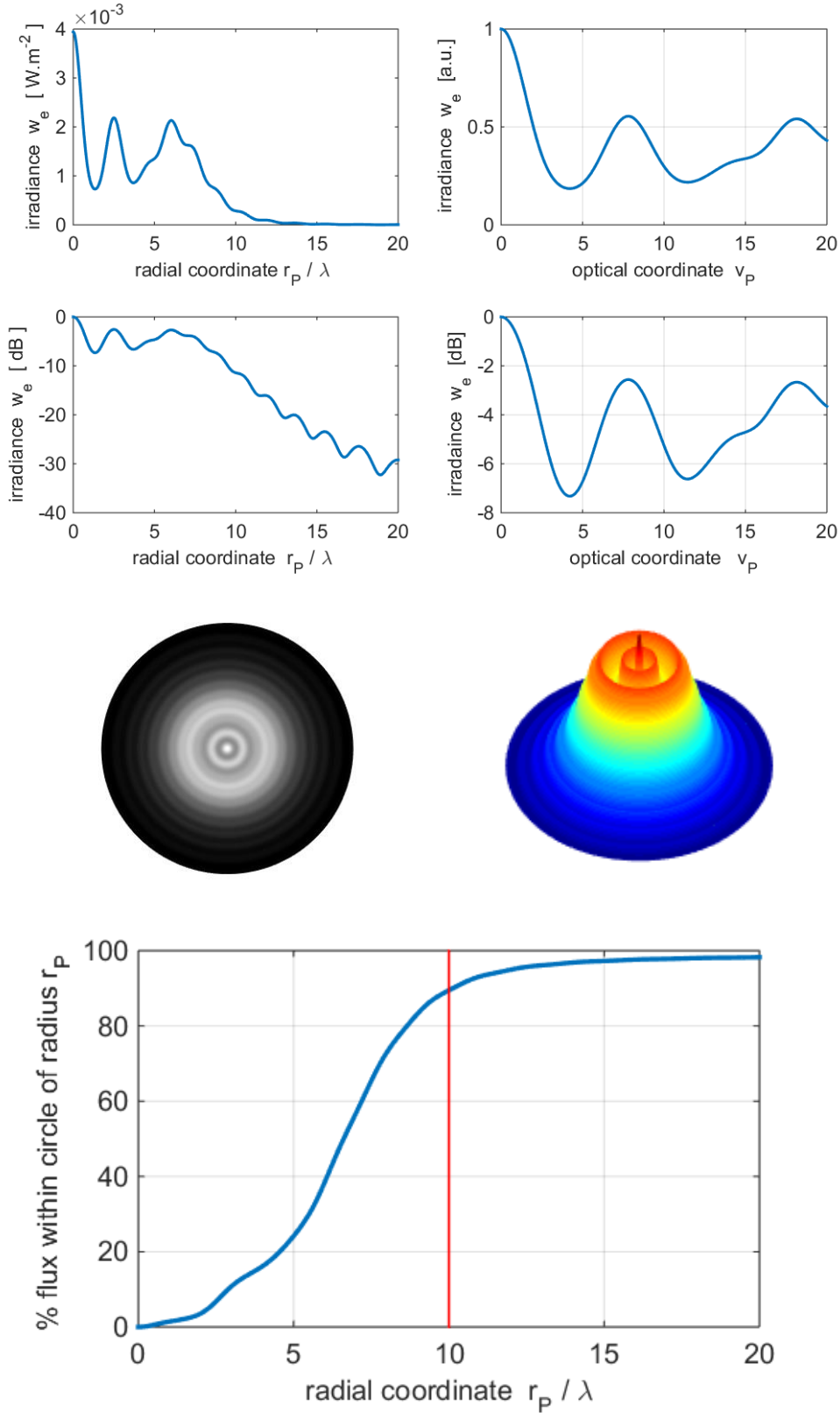

Fig. 4. Diffraction pattern in the near field. $a = 10\,\lambda$ $z_P = 20\,\lambda$
~ 90% of the energy is within a cylinder extended from the aperture with radius *a*. Most of the light has not spread very far from the optical axis but is concentrated directly in front of the aperture.

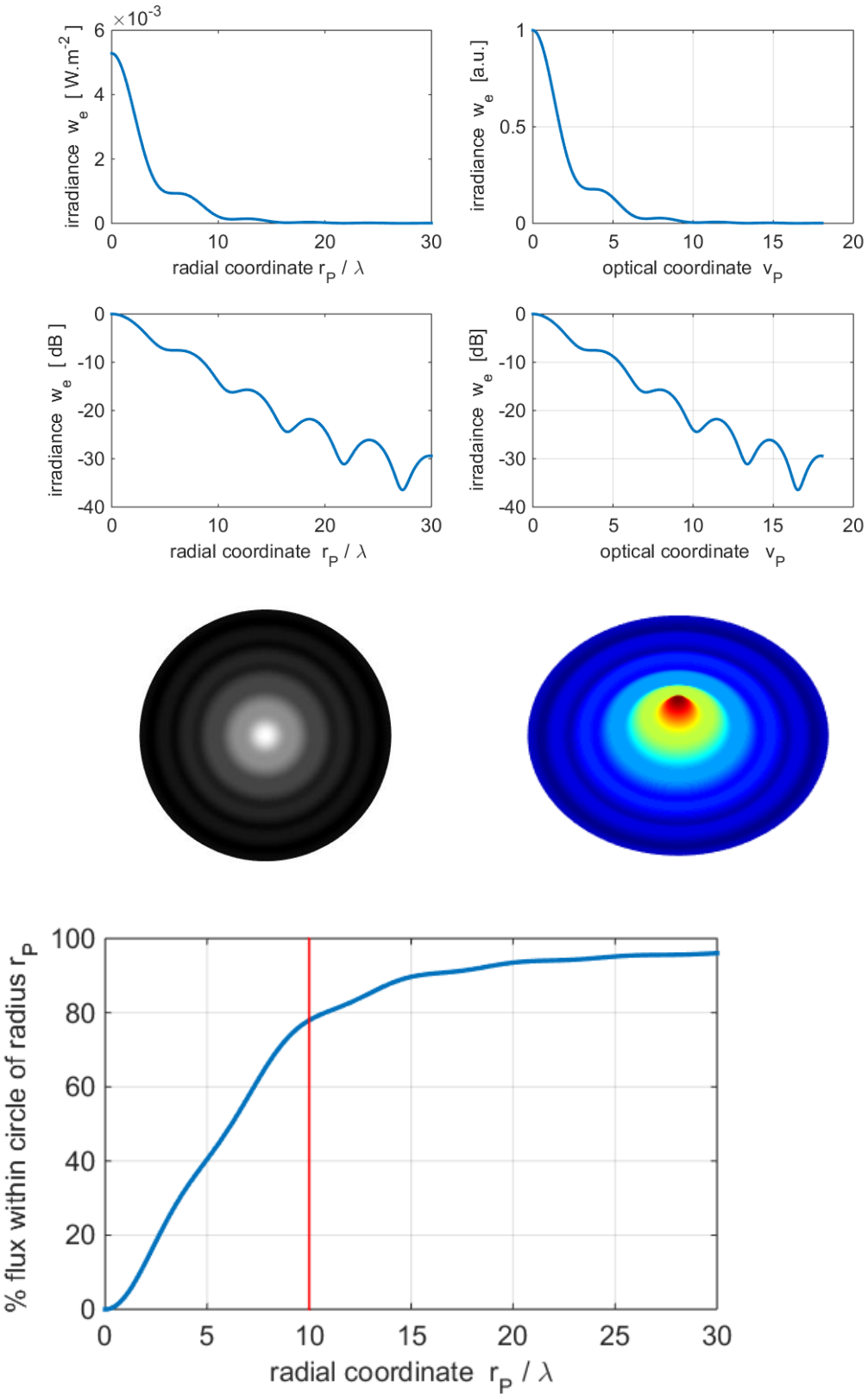

Fig. 5. Diffraction pattern in Fresnel region. $a = 10\,\lambda$ $z_P = 100\,\lambda$ ~ 78% of the energy is within a cylinder extended from the aperture with radius *a*. Most of the light still has not spread very far from the optical axis but is concentrated directly in front of the aperture.

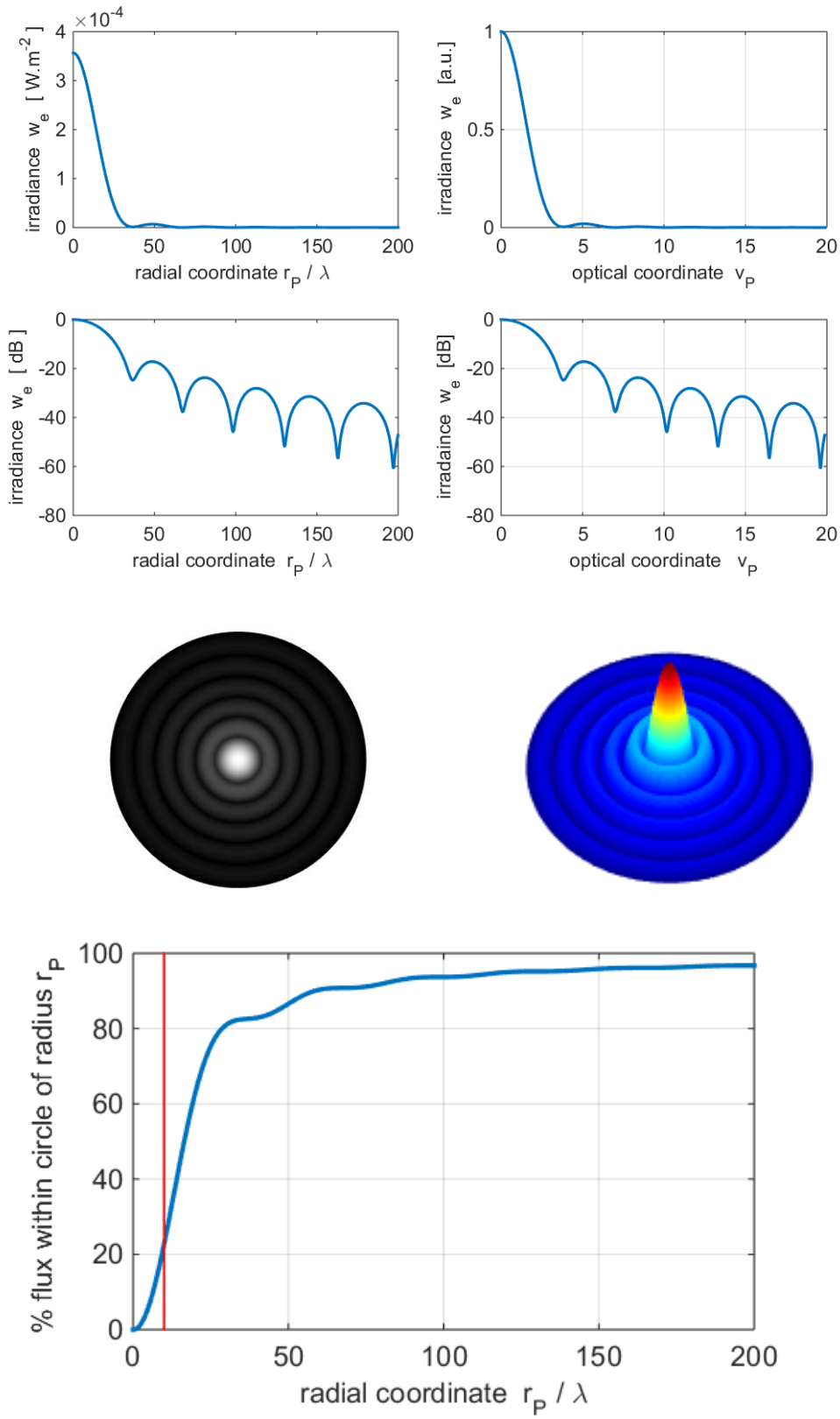

Fig. 6. Diffraction pattern in Fraunhofer region. $a = 10\,\lambda$ $z_P = 600\,\lambda$ ~ 20% of the energy is within a cylinder extended from the aperture with radius *a*. Most of the light has now diffracted away from the optical axis.

We can also model the diffraction pattern for the source close to the aperture. Figure (7) shows the diffraction pattern for the source S(0, 0, -50λ).

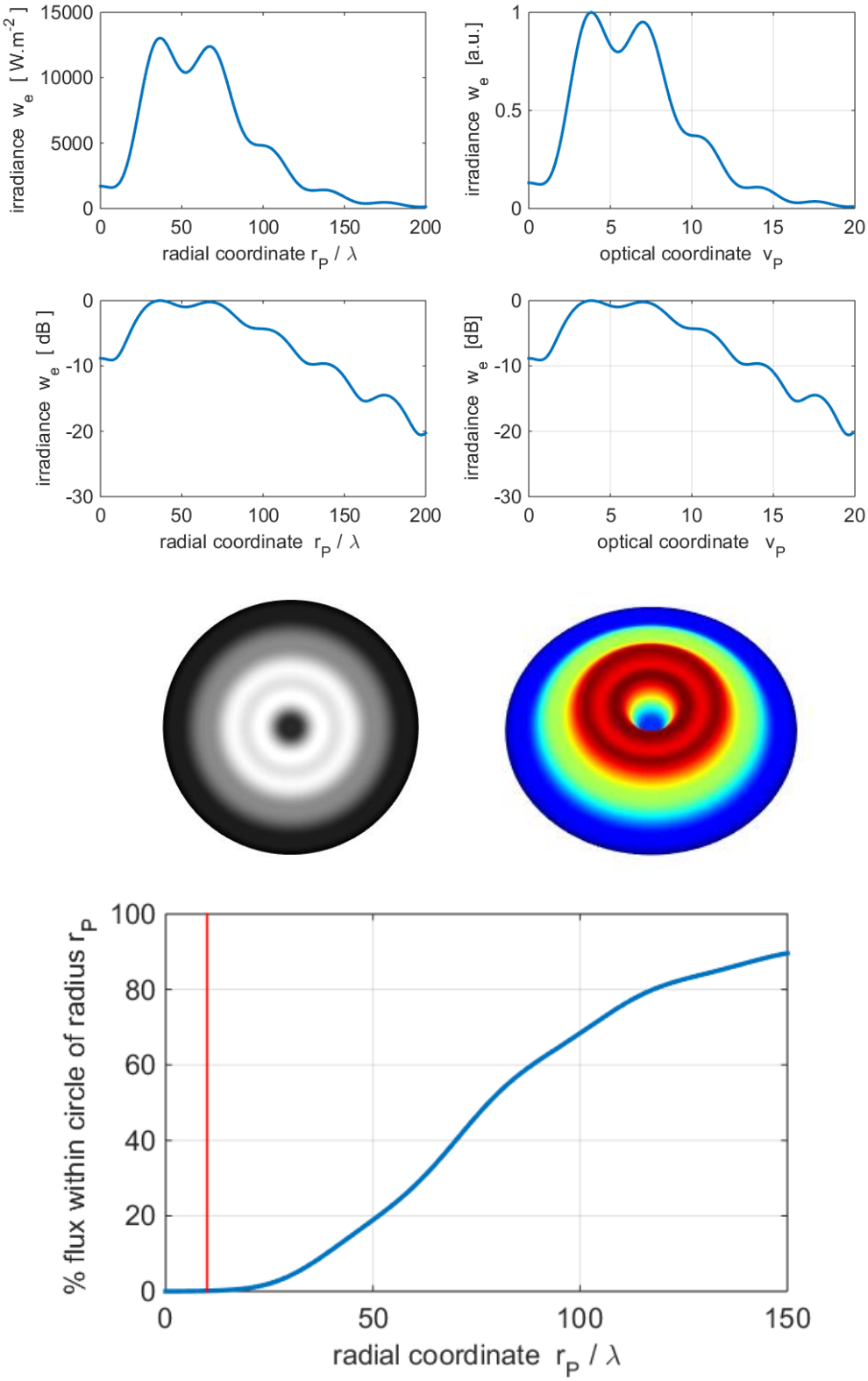

Fig. 7. Diffraction pattern for the source close to the aperture S(0, 0, -50λ). $a = 10\,\lambda$ $z_P = 600\,\lambda$. Irradiance values are very large because the because of the close proximity of the point source to the aperture.

Using a purely numerical technique makes it possible to compute the diffraction field for a much greater variety of situations than would be possible using more traditional analytical methods. For example, the diffracted wave field can be determined for a point source which is not located along the –Z axis.

Figures (8) and (9) show the diffraction patterns from a circular aperture of radius $a = 10\,\lambda$ in the observation plane located at $z_P = 100\,\lambda$ for a source located at $z_S = -50\,\lambda$ using the mscript **op_rs_point_source_xy.m** . Execution time was about 8 minutes for the partitioning of the aperture space n_Q = 24341 and observation space $n_P \times n_P = 221 \times 221 = 48841$. More calculations need to be done using the mscript **op_rs_point_source_xy.m** because in the off-axis case one can't make use of the symmetry properties of the aperture and observation spaces. The plots show scaled values of the irradiance to better emphasize the positions of the minima and maxima.

Figure (8) is for the point source on the optical axis S(0, 0, -50 λ) . Figure (9) is the example for the source located off-axis S(20 λ, 20 λ, -50 λ). The diffraction pattern is characterized by distorted circles surrounding an off-axis bright spot that has a complex structure.

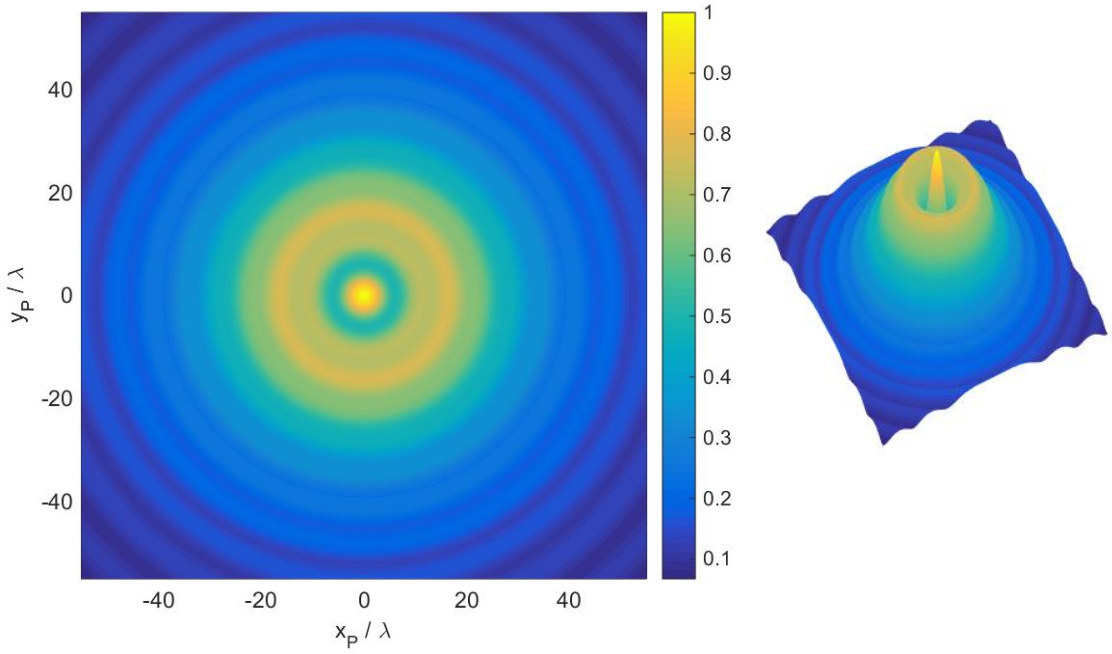

Fig. 8. The radial irradiance for the source located on the optical axis.
λ = 632.8 nm $z_P = 100\,\lambda$ S(0, 0, -50 λ). **op_rs_point_source_xy.m**

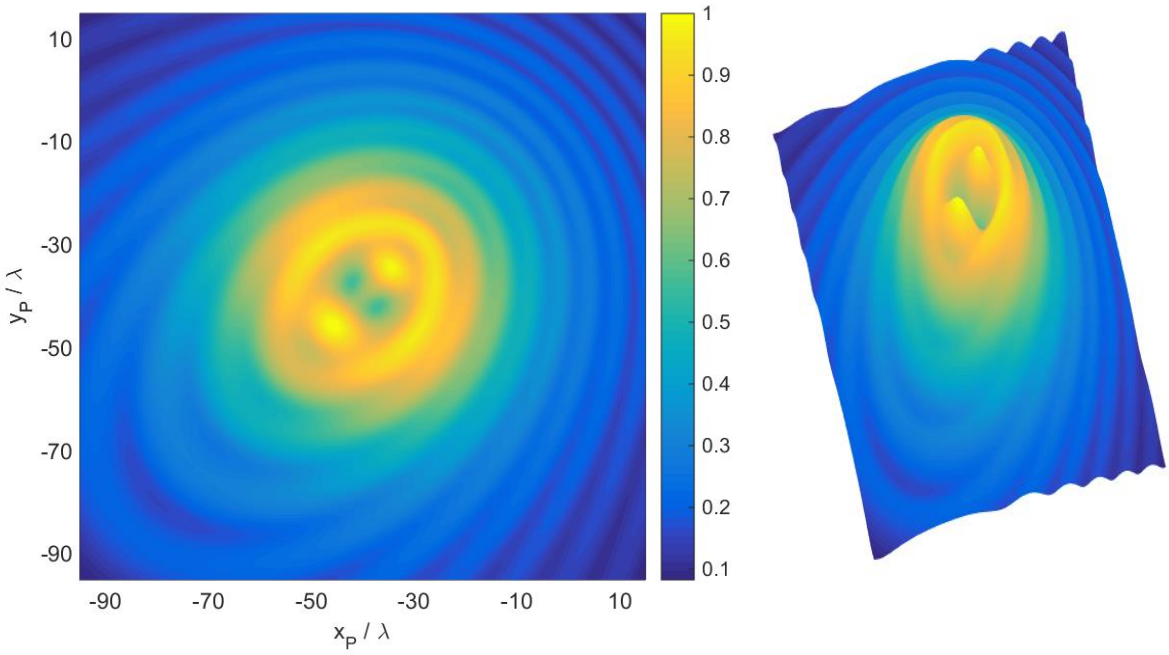

Fig. 9. The radial irradiance for the source located off the optical axis.
λ = 632.8 nm $z_P = 100\,\lambda$ S(20 λ, 20 λ, -50 λ) .
op_rs_point_source_xy.m

Since the irradiance distribution is circularly symmetric about the optical axis, when the circular aperture is illuminated by a point source located on the –Z axis, the irradiance distribution can be displayed in the meridional plane as shown in figure (10). A three-dimensional view can be imagined by rotating the plot in figure (10) about the Z axis.

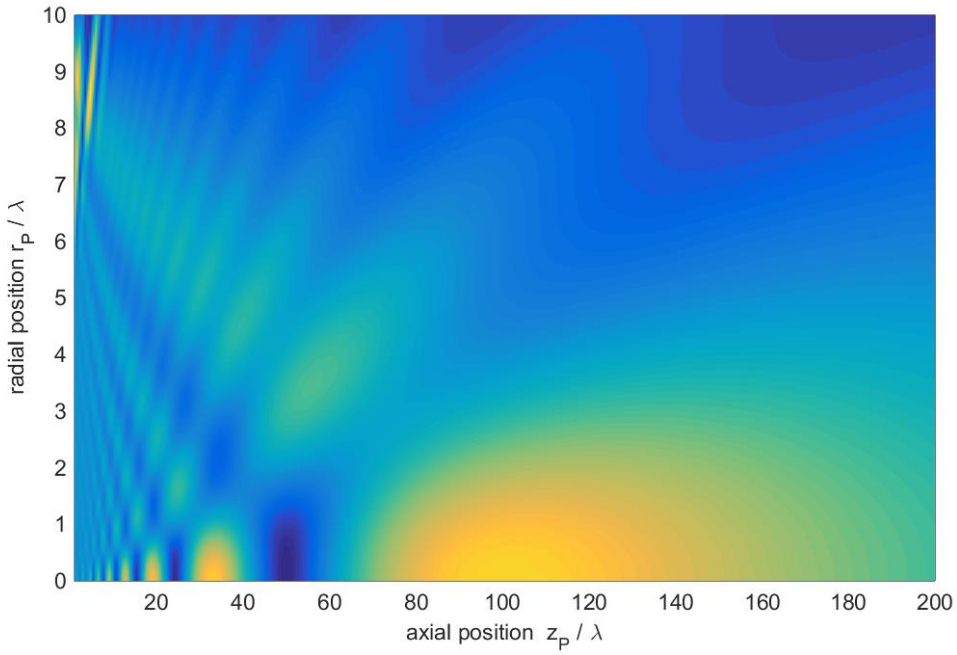

Fig. 10. The irradiance distribution plotted in the meridional plane.
op_rs_point_source_xz.m

The diffracted wave field given by the Rayleigh-Sommerfeld diffraction integral of the first kind is valid over the whole space in front of the aperture, both close and far from the aperture and in regions away from the axis. By having a numerical method of integration that is both accurate and quick, one can eliminate sets of approximations and there is no need for introducing a variety of optical coordinates that are necessary so that the diffraction integrals can be done analytically. The numerical procedure can be used to check many of the approximation methods that have been used in the past. The ability to calculate the near field is also important in investigating the behaviour of near field imaging systems.

Background documents

- Irradiance and radiant flux
- Scalar Diffraction theory: Diffraction Integrals
- Numerical Integration Methods for the Rayleigh-Sommerfeld Diffraction Integral of the First Kind
- View: a more in-depth discussion on the diffraction by circular apertures that are uniformly illuminated (plane wave illumination).

REFERENCES

Barakat R: The calculation of integrals encountered in optical diffraction theory. In Frieden BR (Ed): The computer in optical research, methods and application. pp. 35-80. Springer-Verlag, Berlin 1980

Born M, Wolf E: Principles of Optics, 7th Ed. Cambridge University, Cambridge 1999

Cooper IJ, Sheppard CJR, Sharma M: Numerical integration of diffraction integrals for a circular aperture. Optik, No. 7 (2002) 293-298.

Dubra A, Ferrari JA: Diffracted field by an arbitrary aperture. Am. J. Phys. **67**(1) (1999) 87-92

Forbes GW: Validity of the Frensel approximation in the diffraction of collimated beams. J.Opt.soc.Am.A.**13** (1996) 1816 – 1826

Ganci S: Equivalence between two consistent formulations of Kirchhoff's diffraction theory. J. Opt. Soc. Am. A. **5** (1988) 1626 - 1628

Hsu W, Barakat R: Stratton-Chu vectorial diffraction of electromagnetic fields by apertures with application to small-Fresnel-number systems. J.Opt.soc.Am.A.**11** (1994) 623 – 629

Lindfield G, Penny: Numerical methods using Matlab. Ellishwood, New York 1995

Marchand EW, Wolf E: Consistent formulation of Kirchoff's diffraction theory. J. Opt. Soc. Am. A. **16** (1966) 1712 - 1722

Mendlovic D, Zalevsky Z , Konforti N: Computation considerations and fast algorithms for calculating the diffraction integral. J.Mod.Opt. **44** (1997) 407 - 414

Osterberg H, Smith LW: Closed solutions of Rayleigh's integral for axial points. J. Opt. Soc. **51**(10) (1961) 1050 - 1054

Pozrikidis C: Numerical computation in science and engineering. Oxford University Press 1998

Sheppard CJR, Hrynevych M: Diffraction by a circular aperture: a generalization of Fresnel diffraction theory. J. Opt. Soc. Am. A **9** (1992) 274 - 281

Sheppard CJR, Torok P: Effects of Fresnel number in focussong and imaging. pp. 635 – 649. In Nijhawan OP, Gupta AK, Musla AK, Singh K (Eds): Optics and optoelectronics Vol 1, Narosa Publishing House, New Delhi 1999

Sommerfeld A: Optics – Lectures on theoretical Physics. Vol. 4, pp. 201-217. Academic Press, London 1964

Stamnes JJ: Waves in focal regions. Adam Hilger, Bristol 1986

Steane AM, Rutt HN: Diffraction calculations in the near field and the validity of the Fresnel approximation. J. Opt. Soc. Am. A **6** (1989) pp.1809 – 1814